NANO LETTERS

2008
Vol. 8, No. 8
2580-2584

Enhanced Thermoelectric Figure-of-Merit in p-Type Nanostructured Bismuth Antimony Tellurium Alloys Made from Elemental Chunks

Yi Ma,[†,‡] Qing Hao,[§] Bed Poudel,[†,‡] Yucheng Lan,[†] Bo Yu,[†] Dezhi Wang,[†] Gang Chen,[*,§] and Zhifeng Ren[*,†]

Department of Physics, Boston College, Chestnut Hill, Massachusetts 02467, GMZ Energy, Inc., 12A Hawthorn Street, Newton, Massachusetts 02458, and Department of Mechanical Engineering, MIT, Cambridge, Massachusetts 02139

Received April 7, 2008; Revised Manuscript Received June 4, 2008

ABSTRACT

By ball milling alloyed bulk crystalline ingots into nanopowders and hot pressing them, we had demonstrated high figure-of-merit in nanostructured bulk bismuth antimony telluride. In this study, we use the same ball milling and hot press technique, but start with elemental chunks of bismuth, antimony, and tellurium to avoid the ingot formation step. We show that a peak *ZT* of about 1.3 in the temperature range of 75 and 100 °C has been achieved. This process is more economical and environmentally friendly than starting from alloyed bulk crystalline ingots. The *ZT* improvement is caused mostly by the lower thermal conductivity, similar as the case using ingot. Transmission electron microscopy observations of the microstructures suggest that the lower thermal conductivity is mainly due to the increased phonon scattering from the increased grain boundaries of the nanograins, precipitates, nanodots, and defects. Our material also exhibits a *ZT* of 0.7 at 250 °C, similar to the value obtained when ingot was used. This study demonstrates that high *ZT* values can be achieved in nanostructured bulk materials with ball milling elemental chunks, suggesting that the approach can be applied to other materials that are hard to be made into ingot, in addition to its advantage of lower manufacturing cost.

For several decades, thermoelectric devices have attracted extensive interest because of their excellent features: no moving parts, quiet operation, environmentally friendly, high reliability, and so forth.[1,2] Solid-state thermoelectric devices can be used as direct heat-to-electricity converters (power generation) or as coolers or heat pumps. The efficiency of these devices is determined by a dimensionless figure-of-merit $ZT = (S^2\sigma/k)T$,[3–5] where Z is the figure-of-merit, T is the absolute temperature, S is the Seebeck coefficient, σ is the electrical conductivity, and k is the total thermal conductivity with contributions from the lattice (k_L) and the electrons (k_e). Significant efforts have been made to improve and discover higher ZT materials. One traditional way to improve ZT is to reduce the lattice thermal conductivity k_L via alloying, which does not significantly reduce the electrical properties.

With the application of low dimension concept,[6,7] superlattice Bi_2Te_3/Sb_2Te_3[8] and quantum dot superlattice $PbSe_{0.98}Te_{0.02}/PbTe$[9] have been shown to have significantly improved ZT, mostly because of the reduced k_L. However, it is difficult to scale up these superlattices for large volume energy conversion applications because of limitations in both heat transfer and cost. High ZT values at high temperatures (~500 °C) were reported in bulk materials such as silver antimony lead telluride (LAST)[10,11] synthesized using zone melting and crystal growth technique.

Commercial devices are mostly built on alloys of Bi_2Te_3 and Sb_2Te_3. Such materials, particularly Bi_2Te_3, have a remarkable anisotropy, which originates from the rhombohedral structure composed of quintuple atomic layer series in the order of $Te^{(1)}-Bi-Te^{(2)}-Bi-Te^{(1)}$ along the c axis.[12] Currently, the $Bi_2Te_3-Sb_2Te_3$ alloys are usually prepared by unidirectional crystal growth methods such as zone melting or Bridgman technology.[13,14] Although the resulting crystalline materials present good thermoelectric properties in the plane perpendicular to c axis, they have poor mechanical properties because of weak van der Waals bonding between $Te^{(1)}-Te^{(1)}$ layers. Recently, in order to improve both the thermoelectric and the mechanical properties, we have achieved a peak ZT of 1.4 in p-type $Bi_xSb_{2-x}Te_3$ by ball milling and hot pressing the alloyed crystalline ingot as the

* To whom correspondence should be addressed. E-mail: gchen2@mit.edu (G.C.) and renzh@bc.edu (Z.R.).
† Boston College.
‡ GMZ Energy, Inc.
§ MIT.

10.1021/nl8009928 CCC: $40.75
Published on Web 07/12/2008

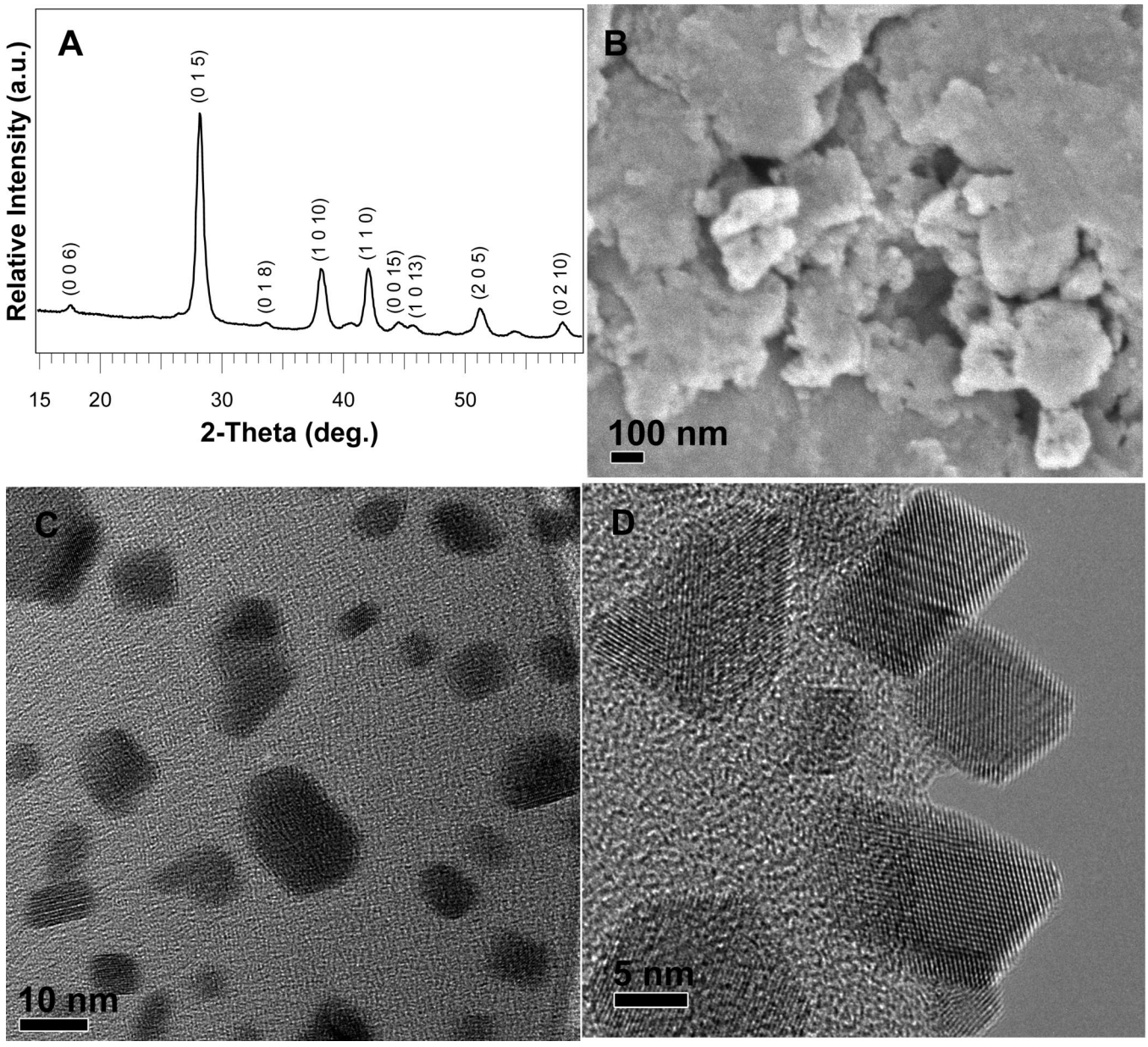

Figure 1. (A) XRD pattern of the nanopowders after ball milling, (B) SEM, (C) bright-field TEM image, and (D) HRTEM image of the mechanically alloyed nanopowders from elements.

starting material,[15] following the suggestion of using a random nanostructuring strategy.[16,17] In this study, we are interested in ball milling elemental chunks of Bi, Sb, and Te into alloy nanopowders first and then hot pressing them into dense bulk to demonstrate a similar high *ZT*.[15] This process eliminates the ingot formation step and is more cost effective and environmentally friendly. A peak *ZT* of about 1.3 in the temperature range of 75 and 100 °C, about 1.1 at room temperature, and 0.7 at 250 °C have been achieved, about 10% lower than those obtained by using ingot as the starting material, probably because of a minor microstructural difference and lack of some minor elements (Zn, Cd, etc.). Such a simple approach should be readily applied to other thermoelectric materials that are hard to be made into crystalline ingot.

Experimental Section. To make nanopowders, appropriate amounts of elemental chunks Bi (99.999%), Sb (99.999%), and Te (99.999%) from Alfa Aesar, were weighed and loaded into a ball mill jar with balls and then subjected to mechanical alloying. To minimize the oxygen contamination, all weighing and loading of the nanopowders were done in a glovebox filled with argon gas. As-prepared nanopowders were then loaded into a graphite die with an inner diameter of 12.7 mm in the glovebox and pressed into bulk disk samples using a direct current induced hot-press in air.[15] As-prepared nanopowders and hot pressed bulk samples were characterized by X-ray diffraction (XRD, Bruker-AXS, G8 GAADS) using Cu Kα radiation, field emission scanning electron microscopy (SEM, JEOL-6340F), transmission electron microscopy (TEM, JEOL-2010F), and a high-resolution TEM (HRTEM).

Disks of 12.7 mm in diameter and 2 mm thick and bars of about 2 × 2 × 12 mm were cut and polished from the pressed disks for the thermoelectric properties characteriza-

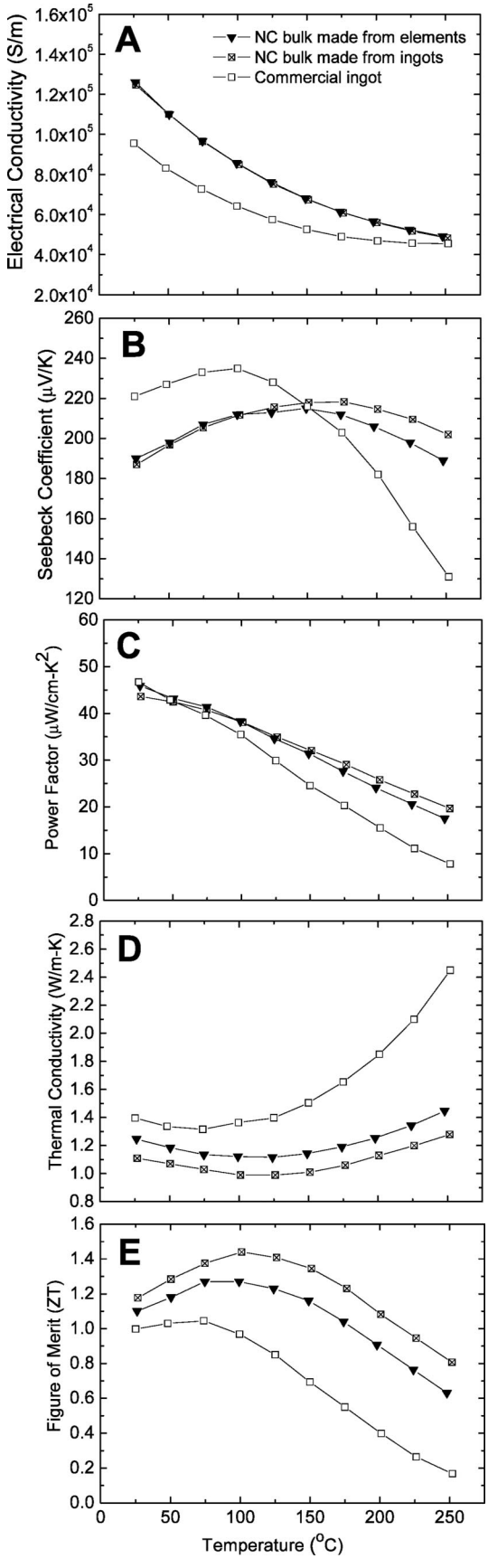

Figure 2. (A) Electrical conductivity, (B) Seebeck coefficient, (C) power factor, (D) thermal conductivity, and (E) *ZT* dependence of temperature of hot-pressed nanocrystalline bulk samples made from elemental chunks in comparison with a commercial ingot[15] and a nanocrystalline bulk sample made from ingot.[15]

tion. The electrical conductivity of the sample was measured by a four-point direct current (dc) current-switching technique, and the Seebeck coefficient was measured by a static dc method based on the slope of the voltage versus temperature-difference curves, using commercial equipment (ZEM-3, Ulvac, Inc.) on the same bar sample cut along the disk plane. The thermal diffusivity was measured by the laser-flash method with a commercial system (LFA 447 Nanoflash, Netzsch Instruments, Inc.). Specific heat was determined by a commercial instrument (DSC 200-F3, Netzsch Instruments, Inc.). We then calculated the thermal conductivity as the product of thermal diffusivity, specific heat, and the volume mass density that was measured by the Archemides technique. Because of the nanograins of our sample, our nanostructured bulk materials are isotropic. To examine the directional dependence of properties, we also pressed samples of 12.7 mm in diameter and 15 mm in thickness so that samples both along and perpendicular to the plane directions were cut and measured. The difference of each property in different directions is within 5%, and the *ZT* is basically the same in different directions, proving the isotropy of the *ZT*s. These results obtained on the commercial characterization systems have been cross-checked using a home-built experimental system that measures all three parameters on the same bar-shaped samples, for which thermal diffusivity is measured using the Angström method.[11]

Results and Discussion. Figure 1 shows the XRD pattern (Figure 1A), SEM image (Figure 1B), bright-field TEM image (Figure 1C), and HRTEM image (Figure 1D) of the nanopowders after ball milling. The XRD pattern verifies that the powders are single phase, indicating that the mechanically assisted reaction during ball milling can make elemental chunks Bi, Sb, and Te into single phase alloy. The broadened diffraction peaks indicate that the particles are small, which is also confirmed by the SEM image (Figure 1B) and low-magnification TEM image (Figure 1C) showing the nanoparticles of about 5 to 20 nm with an average size of about 10 nm. The HRTEM image (Figure 1D) confirms the good crystallinity of the nanoparticles and clean surfaces.

In Figure 2, we compared the transport properties of three types of samples: nanograined sample made from elements, nanograined sample made from crystalline ingot, and the crystalline ingot. The behaviors of the two nanograined samples are similar. The electrical conductivity of the nanograined sample from elements is always higher than that of the crystalline ingot sample (Figure 2A) because of the higher carrier concentration measured by Hall method (Table 1), and it is identical to the nanograined sample made from ingot.[15] The Seebeck coefficient (Figure 2B) of nanograined sample from elements is slightly lower than that from nanograined ingot sample, both of which have a lower Seebeck coefficient than that of the crystalline ingot sample below 150 °C but higher above 150 °C.[15] The smaller Seebeck coefficient near room temperature is due to higher carrier concentration while the larger Seebeck coefficient at higher temperatures is due to suppression of minority carrier (electron) excitation in more heavily doped samples.[18] Figure

Table 1. Mobility and Carrier Concentration at Room Temperature of Our Nanocrystalline Bulk Samples Made from Elemental Chunks in Comparison with the Commercial Ingot and the Nanocrystalline Bulk Samples Made from Ingots

sample	mobility (cm^2/V-sec)	carrier concentration (cm^{-3})
commercial ingot	320 (along *a*-*b* plane) 255 (along *c* direction)	1.8×10^{19}
nanocrystalline bulk made from ingots	264 (uniform all directions)	2.5×10^{19}
nanocrystalline bulk made from elements	273 (uniform all directions)	2.9×10^{19}

2C shows the corresponding power factor of the three samples. The nanograined samples from elements have a power factor comparable to that of the crystalline ingot below 100 °C but higher above 100 °C than that of the ingot, while the nanograined sample from elements has a slightly lower power factor than that made from ingot. Thermal conductivity of the nanograined sample from elements is significantly lower than that of the ingot as expected because of the increased phonon interface scattering, but systematically higher than that of the sample made from ingot,[15] probably because of the lack of some minor elements (Zn, Cd, etc.) that were used in the ingot and a minor structural difference (discussed later).

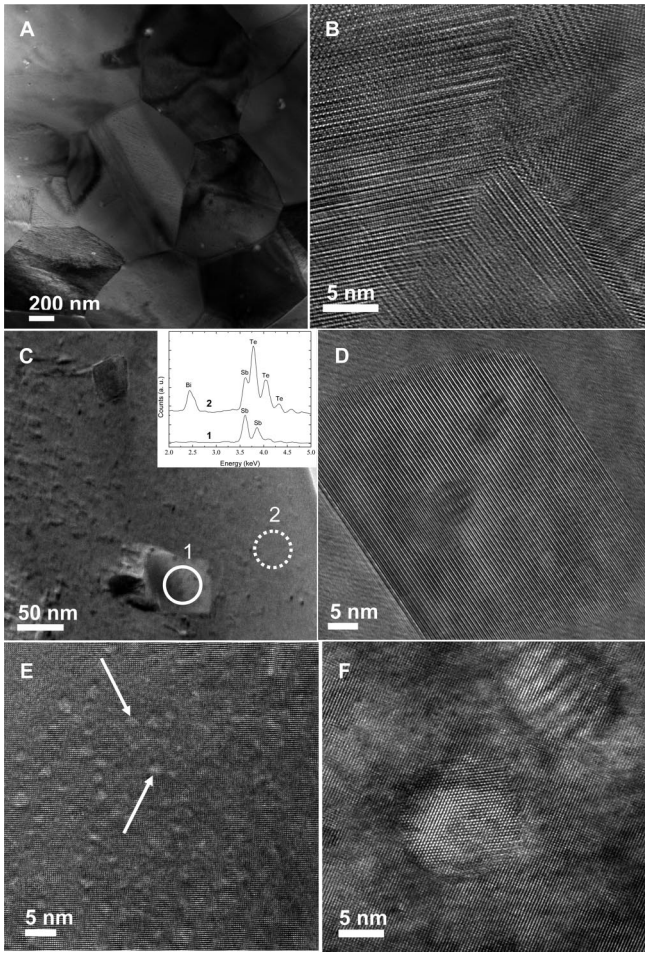

Figure 3. TEM images showing the microstructures of hot-pressed nanocrystalline dense bulk samples made from elemental chunks. (A) low-magnification image showing the submicrometer grains, (B) HRTEM image showing high crystallinity and random orientation, (C) bright-field TEM image and (D) HRTEM image showing Sb precipitates of about 50 nm in the matrix, EDX patterns (inset of Figure 3C) show that the precipitates are pure Sb (marked with 1) and the matrix are BiSbTe alloy. HRTEM images (E,F) showing the nanodots of various sizes (2−3 nm in E indicated by the arrows and 10−15 nm in F) inside the BiSbTe matrix.

Figure 2E shows the temperature dependence of *ZT* for the samples pressed from nanopowders ball milled from elemental chunks in comparison with the commercial ingot and the nanocrystalline bulk sample made from ingot.[15] The peak *ZT* value shifts to a higher temperature and remains significantly higher than that of the ingot at all temperatures, but about 10% lower than that of the nanocrystalline dense bulk made from ingot.[15] The peak *ZT* of our hot pressed samples from elements is about 1.3 in the temperature range of 75 and 100 °C, which is significantly higher than that of the best Bi_2Te_3-based alloy ingots. The superior *ZT* at high temperatures is very important for power generation applications since there are no other materials with a similar high *ZT* at this temperature.

The hot-pressed samples from nanopowders are expected to be isotropic because of the random orientation of the grains.[15] To confirm the isotropic property in the hot-pressed nanocrystalline sample, a thicker disc was prepared and cut both along and perpendicular to the press direction. Each of the three properties is measured and found in agreement within 5%, but the *ZT*s are the same since a higher power factor ($S^2\sigma$, 5%) is always canceled by a similarly higher thermal conductivity (k, 5%).

To understand the mechanism of *ZT* enhancement in hot pressed samples, a TEM investigation of the nanostructure was carried out. The samples were prepared by polishing and ion milling. One of the common features is the presence of submicrometer grains and dense packing as shown in the low magnification TEM image (Figure 3A). An HRTEM image (Figure 3B) shows that grains have excellent crystallinity and large angles between them, which explains isotropy of properties. Although the grains are grown to larger sizes in comparison with the starting nanopowders (Figure 1), each grain shows nanosized features within it. Figure 3C, D clearly shows Sb nanoparticles of sizes up to 50 nm precipitated inside the grains which may occur during the hot press heating and cooling processes. The energy dispersive X-ray spectroscopic (EDX) patterns (inset of Figure 3C) obtained on the precipitates confirm that they are pure Sb. However, we did not see these Sb precipitates, but Te precipitates, in the samples from ingots.[15] Also, we have observed boundaryless nanodots of various sizes that are embedded and dispersed inside the BiSbTe matrix as shown in Figure 3E,F. These two images were taken at different locations of the sample and clearly showed that the sizes are very different: about 2−3 nm (indicated by the arrows) in Figure 3E and 10−15 nm in Figure 3F. These nanodots are formed because of the composition fluctuation inside the grains and are mostly Sb-rich with a typical composition close to Bi:Sb:Te = 9::41:50 with Sb substitution for Te. Both the large size distribution and the high dispersion of the nanodots are favorable to the scattering of a wide spectrum of phonons

(mid-to-long wavelength).[19] We believe that the size of the individual grains, Sb-rich nanodots, and Sb precipitates all help enhance the scattering of the phonons in different energy ranges and therefore contribute to the reduction of the thermal conductivity. The reason why the *ZT* is systematically about 10% lower than the dense nanocrystalline bulk samples made of nanopowders from ball milling the ingot is probably due to lack of some minor elements (Zn, Cd, etc.) that were used in the ingot and also the minor structural difference that Sb instead of Te precipitates in the samples from elements. Experiments on adding extra Te so that Te instead of Sb precipitates form in the matrix are under study to find out whether a further decrease on the thermal conductivity can be achieved. We are also studying whether minor elements such as Zn, Cd, and so forth can further decrease the thermal conductivity.

It is very important to point out that the typical *ZT* values are very repeatable with variations of less than 5% from run to run on more than 100 samples we have run so far for the same composition and processing conditions. A detailed parameters study on composition, ball milling time, hot press temperature, and holding time is under way and will be reported when available.

Conclusions. In summary, we have applied the ball milling and hot press technique to synthesize high *ZT* nanocrystalline bulk thermoelectric materials from elemental chunks Bi, Sb, and Te. A peak *ZT* value of about 1.3 between 75 and 100 °C and of about 0.7 at 250 °C are obtained, similar to what was achieved when ingot was used as the starting materials. By using elemental chunks, the process is significantly simplified in comparison to using of alloyed crystalline ingots. The technique is extendable to other materials that are hard to be made into ingot form, and is also more environmentally friendly since it uses less energy than forming ingot first and then ball milling.

Acknowledgment. This work is supported by DOE DE-FG02-00ER45805 (Z.F.R.), DOE DE-FG02-02ER45977 (G.C.), and NSF NIRT 0506830 (G.C. and Z.F.R.).

References

(1) Disalvo, F. J. *Science* **1999**, *285*, 703.
(2) Sales, B. C. *Science* **2002**, *295*, 1248.
(3) Rowe D. M., Ed., *CRC Handbook of Thermoelectrics* (CRC Press, Boca Raton, FL, 1995).
(4) Goldsmid H. J., *Thermoelectric Refrigeration* (Plenum Press, New York, 1964).
(5) Tritt T. M., Ed., *Semiconductors and Semimetals* (Academic Press, San Diego, CA, 2001).
(6) Hicks, L. D.; Dresselhaus, M. S. *Phys. Rev. B* **1993**, *47*, 12727.
(7) Chen, G. *Phys. Rev. B* **1998**, *57*, 14958.
(8) Venkatasubramanian, R.; Siivola, E.; Colpitts, T.; O'Quinn, B. *Nature* **2001**, *413*, 597.
(9) Harman, T. C.; Taylor, P. J.; Walsh, M. P.; LaForge, B. E. *Science* **2002**, *297*, 2229.
(10) Hsu, K. F.; Loo, S.; Guo, F.; Chen, W.; Dyck, J. S.; Uher, C.; Hogan, T.; Polychroniadis, E. K.; Kanatzidis, M. G. *Science* **2004**, *303*, 818.
(11) Poudeu, P.; D'Angelo, J.; Downey, A.; Short, J. L.; Hogan, T.; Kanatzidis, M. G. *Angew. Chem., Int. Ed.* **2006**, *45*, 3835.
(12) Kitagawa, H.; Nagamori, T.; Tatsuta, T.; Kitamura, T.; Shinohara, Y.; Noda, Y. *Scr. Mater.* **2003**, *49*, 309.
(13) Hyun, D. B.; Oh, T. S.; Hwang, J. S.; Shim, J. D.; Kolomoets, N. V. *Scr. Mater.* **1999**, *40*, 49.
(14) Yamashita, O.; Tomiyoshi, S.; Makita, K. *J. Appl. Phys.* **2003**, *93*, 368.
(15) Poudel, B.; Hao, Q.; Ma, Y.; Lan, Y. C.; Minnich, A.; Yu, B.; Yan, X.; Wang, D. Z.; Muto, A.; Vashaee, D.; Chen, X. Y.; Liu, J. M.; Dresselhaus, M. S.; Chen, G.; Ren, Z. F. *Science* **2008**, *320*, 634.
(16) Yang, R. G.; Chen, G. *Phys. Rev. B* **2004**, *69*, 195316.
(17) Dresselhaus, M. S.; Chen, G.; Tang, M. Y.; Yang, R. G.; Lee, H.; Wang, D. Z.; Ren, Z. F.; Fleurial, J. P.; Gogna, P. *Adv. Mater.* **2007**, *19*, 1043.
(18) Rowe, D. M.; Shukla, V. S.; Savvides, N. *Nature* **1981**, *290*, 765.
(19) Poudeu, P.; D'Angelo, J.; Kong, H. J.; Downey, A.; Short, J. L.; Pcionek, R.; Hogan, T.; Uher, C.; Kanatzidis, M. G. *J. Am. Chem. Soc.* **2006**, *128*, 14347.

NL8009928